Contents

μ-Pro® Mag Documentation

The μ-Pro® Mag program simulates the microstructure evolution of a magnet under applied external magnetic fields, applied strain/stress, and/or electric current. The temporal evolution and spatial profile of magnetization and energies are evaluated.

1 Installation and setup

1.1 Prerequiste

μ-Mag is built with Intel parallel studio cluster edition, and Intel mpi is required to run the program (**libmpi.so.12** and **libmpifort.so.12** are necessary). With Intel mpi installed, if things are not working automatically, you can use the **ldd** command to check the dynamic libraries linked with the executable, and add the correct path for the missing shared library by export **$LD_LIBRARY_PATH**.

1.2 Installation

To install the package, simply run the install.sh script. The script takes one argument, that is the μ-Pro® install path, if no argument is passed, then a default folder **/opt/MUPRO** will be used. For example, if you execute this command **./install.sh /usr/local/MUPRO**. The install.sh script will first create the install directory **/usr/local/MUPRO**, next copy all the contents in your current distribution folder into the install directory, and then add several lines to your **~/.bashrc** file to setup the environment variable **MUPROROOT**, and create alias to the executable for easier usage.

1.3 Using the package

If the package is installed correctly, you should have a set of customized command defined in the ~/.bashrc start with mupro- or copy-mupro-. These commands enable you to execute the program without copy the .exe around.

1.4 Activate your usage

To register your copy of the program, we need the following information:

1. Hostname. Be careful that this may not be the host name you used to get access to your linux server, but the host name of the login node you get connected to. For example, I can connect to the Penn State server through **ssh xuc116@aci-b.aci.ics.psu.edu**, but due to there are multiple login nodes, I'm actually connected to a node called **aci-004.aci.production.int.aci.ics.psu.edu**. This is the host name you should provide to us, rather than the **aci-b.aci.ics.psu.edu** one. If there are more than one hostname that you may get connected to you can supply us with a list of them. You can easily obtain the hostname of your server or computer by execute **echo $HOSTNAME** in the linux terminal.
2. Username. The user name you want to grant access to use μ-Mag. You can find the user name by typing **echo $USER** in the terminal. Note if you apply for the group license rather than individual one, you should provide the group name instead of user name.
3. Groupname. The group of users that you want to grant access to use μ-Mag. You can find all of the group you belong to by executing the **id** command in terminal.
4. Ip address. You can obtain your server's ip address by typing **curl ipinfo.io/ip** in terminal. Same as hostname, if there are more than one ip address that you may get connected to, you can provide us with a list of them.

2 Simulation Method

2.1 Basic design

The total size of the simulation system is $l_1 \times l_2 \times l_3$, which is evenly discretized into $n_1 \times n_2 \times n_3$ cuboid grids, i.e., the size of each simulation grid is $\Delta l_1 = l_1/n_1$, $\Delta l_2 = l_2/n_2$, and $\Delta l_3 = l_3/n_3$.

The simulation system can be one of the following types:
Bulk, 3-D;
Bulk, 2-D;
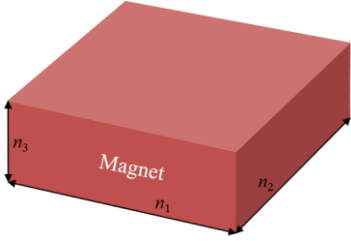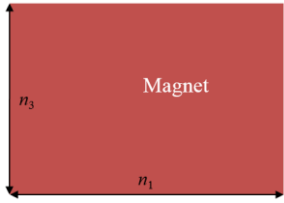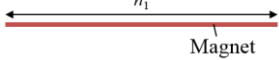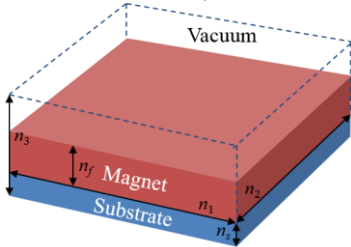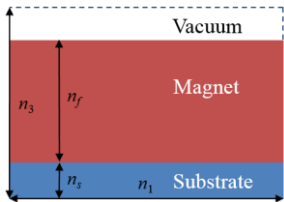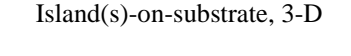Bulk, 1-D;
Thin film, 3-D;
Thin film, 2-D;
Island-on-substrate, 3-D;
Island-on-substrate, 2-D;
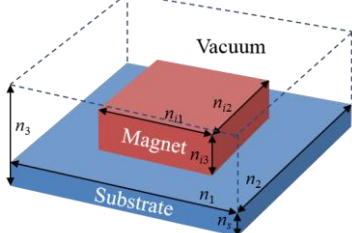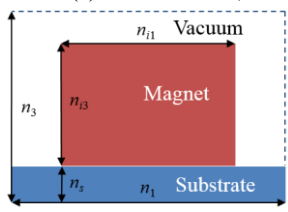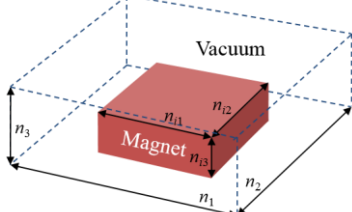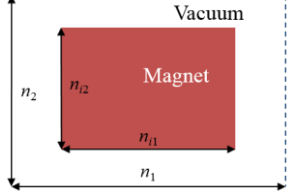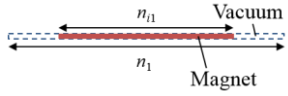
Freestanding finite-size magnet, 3-D;
Freestanding finite-size magnet, 2-D;
Freestanding finite-size magnet, 1-D.

A set of additional parameters are used to specify the system, which may include the film thickness n_f, island (or finite-size magnet) thickness n_{i3}, island (or finite-size magnet) lengths n_{i1} and n_{i2}, and substrate thickness n_s. Schematics of all types of systems and corresponding parameters are listed below. All the parameters are in the unit of grid numbers.

Table 2.1 Types of systems

System type and schematics	Parameters specifying the system	Value of parameters
Bulk, 3-D	n_1	Length of the system along x_1 direction
	n_2	Length of the system along x_2 direction
	n_3	Length of the system along x_3 direction
	n_f	0
	n_{i3}	0
Bulk, 2-D	n_1	Length of the system along x_1 direction
	n_2	1*
	n_3	Length of the system along x_3 direction
	n_f	0
	n_{i3}	0
Bulk, 1-D	n_1	Length of the system along x_1 direction
	n_2	1*
	n_3	1
	n_f	0
	n_{i3}	0
Thin film, 3-D	n_1	Length of the system along x_1 direction
	n_2	Length of the system along x_2 direction
	n_3	Length of the system along x_3 direction
	n_f	Thickness of the film along x_3 direction
	n_s	Thickness of the substrate along x_3 direction
Thin film, 2-D	n_1	Length of the system along x_1 direction
	n_2	1*
	n_3	Length of the system along x_3 direction
	n_f	Thickness of the film along x_3 direction
	n_s	Thickness of the substrate along x_3 direction
Island(s)-on-substrate, 3-D	n_1	Length of the system along x_1 direction
	n_2	Length of the system along x_2 direction

5

	Parameter	Description
	n_3	Length of the system along x_3 direction
	n_f	0
	n_{i3}	Thickness of the island along x_3 direction
	n_s	Thickness of the substrate along x_3 direction
	C_{Island}	1
	n_{i1}	Length of the island along x_1 direction
	n_{i2}	Length of the island along x_2 direction

Island(s)-on-substrate, 2-D

Parameter	Description
n_1	Length of the system along x_1 direction
n_2	1*
n_3	Length of the system along x_3 direction
n_f	0
n_{i3}	Thickness of the island along x_3 direction
n_s	Thickness of the substrate along x_3 direction
C_{Island}	1
n_{i1}	Length of the island along x_1 direction
n_{i2}	1*

Freestanding finite-size magnet, 3-D

Parameter	Description
n_1	Length of the system along x_1 direction
n_2	Length of the system along x_2 direction
n_3	Length of the system along x_3 direction
n_f	0
n_{i3}	Thickness of the magnet along x_3 direction
n_s	0
C_{Island}	1
n_{i1}	Length of the magnet along x_1 direction
n_{i2}	Length of the magnet along x_2 direction

Freestanding finite-size magnet, 2-D

Parameter	Description
n_1	Length of the system along x_1 direction
n_2	Length of the system along x_2 direction
n_3	1
n_f	0
n_{i3}	1
n_s	0
C_{Island}	1
n_{i1}	Length of the magnet along x_1 direction
n_{i2}	Length of the magnet along x_2 direction

Freestanding finite-size magnet, 1-D

Parameter	Description
n_1	Length of the system along x_1 direction
n_2	1*
n_3	1
n_f	0
n_{i3}	1
n_s	0
C_{Island}	1
n_{i1}	Length of the magnet along x_1 direction
n_{i2}	1*

* There's a limit of $n_2 \geq 2$ in simulation running parallel with multiple processors, where n_2 ($= n_{i2}$) = 2 is recommended in quasi- 2-D or 1-D systems.

C_{Island} on input specifies whether the in-plane (i.e., in x_1-x_2 plane) shape of an island or a freestanding finite-size magnet be a rectangle ($C_{\text{Island}}=1$), an ellipse ($C_{\text{Island}}=2$), or any other arbitrary shape ($C_{\text{Island}}=0$), respectively. On setting $C_{\text{Island}}=2$, n_{i1} and n_{i2} would specify the major or minor axes of the ellipse along x_1 and x_2 directions, respectively. On setting $C_{\text{Island}}=0$, an arbitrary

in-plane shape defined in an input file *islandShape.in* would be adopted (see Section 3 for details). Cases for $C_{Island}=2$ and $C_{Island}=0$ are omitted in Table 2.1.

For thin films and island(s)-on-substrate systems, the thickness of the substrate should be at least 11 grids, i.e., $n_s \geq 11$. At all actual surfaces of a magnet, a number of at least 4 stacking layers of vacuum is needed, if one or more of the following components is considered: (demagnetizing) stray field, magnetoelastic interaction, exchange interaction, or Dzyaloshinskii-Moriya interaction (DMI). For example, for simulating a cuboid island with a length of n_{i1} grids along x_1 direction, n_1 should be chosen following $(n_1 - n_{i1})/2 \geq 4$.

Spatial distribution of the local magnetization vector $\mathbf{M}(\mathbf{x}) = M_S \mathbf{m}(\mathbf{x})$ is used to describe magnetic domain structure, where $\mathbf{x}$ is the position vector, M_S is the spontaneous magnetization, and $\mathbf{m}$ is the normalized magnetization. The SI units are adopted in μ-Pro$^\circledR$ Mag and throughout this documentation.

A set of Euler angle arrays including $\varphi(\mathbf{x})$, $\theta(\mathbf{x})$, and $\psi(\mathbf{x})$ are introduced to treat a polycrystal. These angle arrays rotate the system coordinate axes to the local crystallographic coordinate axes. The transformation matrix $\mathbf{a}$ from the system coordinates to the local crystallographic coordinates is

$$\mathbf{a} = \begin{pmatrix} \cos\varphi\cos\psi - \cos\theta\sin\varphi\sin\psi & \cos\theta\cos\varphi\sin\psi + \sin\varphi\cos\psi & \sin\theta\sin\psi \\ -\cos\theta\sin\varphi\cos\psi - \cos\varphi\sin\psi & \cos\theta\cos\varphi\cos\psi - \sin\varphi\sin\psi & \sin\theta\cos\psi \\ \sin\theta\sin\varphi & -\sin\theta\cos\varphi & \cos\theta \end{pmatrix} \quad (1)$$

For example, transformation of a vector $\mathbf{v}$ from the system coordinates to local crystallographic coordinates follows $v_{i'} = a_{ij} v_j$ (i,j=1,2,3). Here a prime (') in a subscript following an index 1, 2, or 3 indicates a component of a vector or a tensor in the local crystalline coordinate, e.g., $m_{1'}(\mathbf{x})$ is the component of $\mathbf{m}(\mathbf{x})$ along the local crystallographic coordinate axis x_1' at position $\mathbf{x}$. Note that Einstein summation convention is adopted throughout the documentation.

2.2 Magnetization dynamics

Temporal evolution of $\mathbf{m}$ is governed by the Landau-Lifshitz-Gilbert (LLG) equation, i.e.,

$$\frac{\partial \mathbf{m}}{\partial t} = \tau = -\frac{\gamma_0}{1+\alpha^2} \left(\mathbf{m} \times \mathbf{H}_{eff} + \alpha \mathbf{m} \times (\mathbf{m} \times \mathbf{H}_{eff}) \right), \quad (2)$$

where t is the time, τ is the total torque, α is the damping constant, γ_0 is the gyromagnetic ratio in $m/(A \cdot s)$. $\mathbf{H}_{eff}$ is the effective magnetic field, which includes the following contributions:

- External field $\mathbf{H}_{ext}$;
- Magnetic stray field or demagnetizing field $\mathbf{H}_d$;
- Magnetocrystalline anisotropy field $\mathbf{H}_{anis}$;
- Magnetoelastic field $\mathbf{H}_{elas}$;
- Exchange interaction field $\mathbf{H}_{exch}$;

- Dzyaloshinskii-Moriya interaction (DMI) field $\mathbf{H}_{DMI}$;
- Effective field from spin-transfer torque or spin-orbit torque $\mathbf{H}_{ST}$,
- Thermal fluctuation field $\mathbf{H}_{therm}$;

as below,

$$\mathbf{H}_{eff} = \mathbf{H}_{ext} + \mathbf{H}_{stray} + \mathbf{H}_{anis} + \mathbf{H}_{elas} + \mathbf{H}_{exch} + \mathbf{H}_{DMI} + \mathbf{H}_{ST} + \mathbf{H}_{therm}. \tag{3}$$

$\mathbf{H}_{eff}$ is given by

$$\mathbf{H}_{eff} = -\frac{1}{\mu_0}\frac{\delta F[\mathbf{M}]}{\delta \mathbf{M}} + \mathbf{H}_{therm}. \tag{4}$$

where $\mu_0 = 4\pi \times 10^{-7}\,\text{N/A}^2$ is the vacuum permeability, $F[\mathbf{M}] = \int f[\mathbf{M}]d\mathbf{x}^3$ is the Helmholtz free energy of the system, as a functional of the magnetization distribution, where f is the volume density of the Helmholtz free energy, given by

$$f = f_{ext} + f_{stray} + f_{anis} + f_{elas} + f_{exch} + f_{DMI} + f_{ST}. \tag{5}$$

μ-Pro® Mag provides two numerical methods for solving the LLG equation:
- IGS, implicit Gauss-Seidel projection method[1] implemented with Fourier-Spectral approach[2][3]. Contribution of the short-range interaction $\mathbf{H}_{exch}$ is implicitly considered, while other contributions to $\mathbf{H}_{eff}$ are explicitly evaluated.
- RK4, the Runge-Kutta method. All contributions to $\mathbf{H}_{eff}$ are explicitly evaluated.

The time during magnetization evolution is discretized into time steps with a fixed duration Δt, i.e., $t = k_t \Delta t$ where k_t is the step number. The recommended range for the value of Δt is $10^{-14}\,\text{s} \le \Delta t \le 10^{-12}\,\text{s}$, for numerical stability and accuracy.

2.3 External field, stray field, and magnetostatic boundary condition

The magnetic field $\mathbf{H}$ consists of external field and magnetostatic stray field, i.e., $\mathbf{H} = \mathbf{H}_{ext} + \mathbf{H}_{stray}$. In μ-Pro® Mag, the external field $\mathbf{H}_{ext}$ is considered spatially uniform in the simulation system, in the unit of A/m. The volume density of external field energy is given by

$$f_{ext} = -\mu_0 M_S \mathbf{H}_{ext} \cdot \mathbf{m}. \tag{6}$$

μ-Pro® Mag provides an option of choosing $\mathbf{H}_{ext}$ on input as a combination of a DC and an AC component, i.e., $\mathbf{H}_{ext} = \mathbf{H}_{DC} + \mathbf{H}_{AC}\sin(2\pi f_{AC} \cdot t)$

The magnetostatic stray field energy is given by

$$F_{stray} = \int_{\text{entire space}} \frac{1}{2}\mu_0 \mathbf{H}_{stray}^2 d\mathbf{x}^3 = \int_{\text{magnet}} -\frac{1}{2}\mu_0 M_S \mathbf{H}_{stray} \cdot \mathbf{m}d\mathbf{x}^3. \tag{7}$$

The energy density is taken as

$$f_{stray} = -\frac{1}{2}\mu_0 M_S \mathbf{H}_{stray} \cdot \mathbf{m}. \tag{8}$$

$\mathbf{H}_{\text{stray}}$ is obtained at each evolution step by solving the magnetostatic equilibrium equation

$$\nabla \cdot (\mathbf{H} + \mathbf{M}) = 0. \tag{9}$$

Three types of boundary condition are used for $\mathbf{H}_{\text{stray}}$. In a period boundary condition, the simulation system is considered as a building block that appears repeatedly appear in 3-D space, and the stray field is expressed as $\mathbf{H}_{\text{stray}} = -\nabla\phi + \mathbf{N}_D \overline{\mathbf{M}}$, where ϕ is the magnetic scalar potential with a periodic boundary condition solved using the Fourier spectral method, as given in Ref. [3], the 3×3 symmetric matrix $\mathbf{N}_D$ is the demagnetizing factor which depends only on the macroscopic shape of the actual sample (not the shape of the simulation system, e.g., see Table 2.2), and $\overline{\mathbf{M}}$ is the average magnetization of the simulation system. In a finite-size boundary condition, space outside the simulation system is considered to be filled by vacuum without magnetization, electric charge, or current etc., and the stray field is solved based on convolution theorem accelerated by FFT[4], without explicitly utilizing demagnetizing factors. The third type of boundary condition is a mixed type which considers periodic boundaries along in-plane directions x_1 and x_2, and finite-size boundaries along the out-of-plane direction x_3, which is solved using Fourier spectral method, without utilizing demagnetizing factors. Table 2.2 lists the recommended stray field boundary conditions and (when applicable) demagnetizing factors for typical types of systems.

Table 2.2 Recommended stray field boundary condition and demagnetizing factor

System type	Boundary condition	(N_{D1}, N_{D2}, N_{D3})
Bulk (periodic)	Periodic	(0, 0, 0) or (1/3, 1/3, 1/3), or calculated based on the macroscopic shape of the sample
Thin film (periodic in-plane)	Mixed	/
Island(s)-on-substrate arrays (periodic in-plane)	Mixed	/
Single group of island(s)-on-substrate	Finite-size	/
Freestanding finite-size magnet	Finite-size	/

2.4 Magnetocrystalline anisotropy

Two types of magnetocrystalline anisotropy are considered, the cubic anisotropy with magnetic easy axes along <100>, <110>, or <111> crystal axes, and the uniaxial anisotropy in ultra-thin films with a magnetic easy/hard axis perpendicular to the film plane. The volume density of magnetocrystalline anisotropy energy is given by

Cubic anisotropy

$$f_{\text{anis}} = K_1 \left(m_{1'}^2 m_{2'}^2 + m_{1'}^2 m_{3'}^2 + m_{2'}^2 m_{3'}^2 \right) + K_2 m_{1'}^2 m_{2'}^2 m_{3'}^2 + K_3 \left(m_{1'}^4 m_{2'}^4 + m_{1'}^4 m_{3'}^4 + m_{2'}^4 m_{3'}^4 \right) \tag{10A}$$

Uniaxial anisotropy

$$f_{\text{anis}} = K_1 \left(1 - m_3^2 \right) + K_2 \left(1 - m_3^2 \right)^2 \tag{10B}$$

where $\mathbf{K}$ is the magnetocrystalline anisotropy coefficient.

The anisotropy effective field is calculated as

9

$$\mathbf{H}_{\text{anis}} = -\frac{1}{\mu_0 M_S} \frac{\partial f_{\text{anis}}}{\partial \mathbf{m}} \tag{11}$$

2.5 Magneto-Elastic interaction

The elastic energy density is given by

$$f_{\text{elas}} = \frac{1}{2} \mathbf{c} \left(\mathbf{\varepsilon} - \mathbf{\varepsilon}^0 \right)^2 \tag{12}$$

where $\mathbf{c}$ is the elastic stiffness tensor, $\mathbf{\varepsilon}$ is the strain, and $\mathbf{\varepsilon}^0$ is the stress-free strain calculated as

$$\mathbf{\varepsilon}^0_{i'j'} = \begin{cases} \dfrac{3}{2} \lambda_{100} \left(m_{i'}^2 - \dfrac{1}{3} \right) & (i' = j') \\ \dfrac{3}{2} \lambda_{111} m_{i'} m_{j'} & (i' \neq j') \end{cases} \tag{13}$$

where λ_{100} and λ_{111} are saturation magnetostriction along <100> and <111> crystalline axes, respectively.

The magnetoelastic effective field is written as

$$\mathbf{H}_{\text{elas}} = -\frac{1}{\mu_0 M_S} \frac{\partial f_{\text{elas}}}{\partial \mathbf{m}} = \frac{2\mathbf{\sigma}}{\mu_0 M_S} \cdot \frac{\partial \mathbf{\varepsilon}^0}{\partial \mathbf{m}} \tag{14}$$

where $\mathbf{\sigma}$ is the stress field given by $\mathbf{\sigma} = \mathbf{c} \left(\mathbf{\varepsilon} - \mathbf{\varepsilon}^0 \right)$.

Assuming that the elastic equilibrium condition holds at each evolution step, the strain and stress are obtained at each evolution step through solving the mechanical equilibrium equation

$$\nabla \cdot \mathbf{\sigma} = 0 \tag{15}$$

using a Fourier spectral method[5][6] based on Khachaturyan's elasticity theory[7]. Table 2.3 summarizes the boundary conditions implemented in typical types of systems. Examples showing the influence of elastic boundary condition on the magnetic domain structure can be found in Ref.[8].

Table 2.3 Elastic boundary conditions

System type	Boundary condition
Bulk (periodic)	3-d periodic, with specified applied external strain ε_{ext} or stress σ_{ext}
Thin film (periodic in-plane)	Thin film boundary condition (see Ref. [5] for details), with specified in-plane substrate strain ε_{ext} (i.e., $\varepsilon_{\text{ext11}}$, $\varepsilon_{\text{ext22}}$, and $\varepsilon_{\text{ext12}}$)
Island(s)-on-substrate	Periodic in-plane, stress-free island surfaces, with specified in-plane substrate strain ε_{ext} (i.e., $\varepsilon_{\text{ext11}}$, $\varepsilon_{\text{ext22}}$, and $\varepsilon_{\text{ext12}}$)
Freestanding finite-size magnet	Stress-free

An iterative Fourier-Spectral method is used (see details in Ref. [6]) to solve Eq. 15 in elastically inhomogeneous systems (that is, spatially variant $\mathbf{c}$), including:

- Island-on-substrate system
- freestanding finite-size systems
- Polycrystals

- Film-on-substrate system where the magnet and substrate have different elastic stiffness.

A convergence of the iterative approximation is claimed when the difference of total elastic energy between adjacent recursion loops is within a tolerance value Δe (arbitrary unit), i.e., $\left| F_{elas}^{(n)} - F_{elas}^{(n-1)} \right| \leq \Delta e$, where $F_{elas}^{(n)}$ is the total elastic energy of the n-th iterative approximation. If convergence is not reached after the allowed maximum number n_{Recurs} of recursion loops, the program claims to fail to solve the mechanical equilibrium equation and stops. Both n_{Recurs} and Δe are user adjustable (see Section 3) with recommended range of 100~2000 and 10^{-5}~10^{-3}, respectively. To speed up the iteration process, a solved strain distribution of the initial time step can be provided within input, and used as the starting approximation of the first iterative loop.

2.6 Magnetic exchange interaction

The density of magnetic exchange energy is given by
$$f_{exch} = A\left((\nabla m_1)^2 + (\nabla m_2)^2 + (\nabla m_3)^2 \right) = A(\nabla \mathbf{m})^2 \tag{16}$$
where A is the exchange constant in the unit of J/m.

The exchange field is expressed as
$$H_{exch} = \frac{2A}{\mu_0 M_S} \nabla^2 \mathbf{m} \tag{17}$$

2.7 Dzyaloshinskii-Moriya interaction (DMI)

The DMI module in μ-Pro® Mag belongs to the interface type[9], which can be invoked when simulating an ultrathin magnetic thin film or island with perpendicular magnetic anisotropy. Consider a homogenous effective DMI constant D, the interface DMI energy density is given by
$$f_{DMI} = D\left(m_3 \nabla \mathbf{m} - \mathbf{m} \cdot \nabla m_3 \right) \tag{18}$$

The effective magnetic field due to DMI is therefore expressed as
$$H_{DMI} = \frac{2D}{\mu_0 M_S} \left(\nabla m_3 - \mathbf{e_3} \nabla \cdot \mathbf{m} \right) \tag{19}$$
where $\mathbf{e}_3$ is the unit vector along the x_3 direction.

2.8 Spin torque

The spin-orbit torque and Slonczewski spin-transfer torque are given by
$$\boldsymbol{\tau}_{ST} = \frac{\tau_0}{1+\alpha^2} \left(\mathbf{m} \times (\mathbf{m}_P \times \mathbf{m}) - \alpha (\mathbf{m}_P \times \mathbf{m}) \right) \tag{20}$$

where $\mathbf{m}_P$ is the normalized fixed-layer magnetization in the case of spin-transfer torque, while represents the direction of spin current generated through Spin Hall Effect; and the pre-factor τ_0 depends on the type of the spin torque.

For spin-orbit torque[10],

$$\tau_0 = \frac{\mu_B J \theta_{\mathrm{SH}}}{edM_S} \tag{21}$$

where $\mu_B = 9.27400968 \times 10^{-24} \mathrm{A \cdot m^2}$ is the Bohr magneton, J is the electric current density, θ_{SH} is the spin Hall angle, $e = 1.6021766209 \times 10^{-19} \mathrm{C}$ is the elementary charge. d is the thickness of the free magnetization layer, as defined with the type of the system (see Table 2.1).

For Slonczewski spin-transfer torque[11][12],

$$\tau_0 = \frac{2\mu_B J}{edM_S} \left(-4 + \frac{\left(1+\eta_{\mathrm{SP}}\right)^3 \left(3 + \mathbf{m} \cdot \mathbf{m}_P\right)}{4\eta_{\mathrm{SP}}^{3/2}} \right)^{-1} \tag{22}$$

where η_{SP} is the spin polarization constant.

The effective field corresponding to spin-orbit torque or Slonczewski spin-transfer torque is given by

$$\mathbf{H}_{\mathrm{ST}} = \frac{\tau_0}{\gamma_0} \left(\mathbf{m} \times \mathbf{m}_P \right) \tag{23}$$

The Zhang-Li spin-transfer torque is given by[13]

$$\boldsymbol{\tau}_{\mathrm{ST}} = \frac{1}{1+\alpha^2} \frac{\mu_B}{2eM_S\left(1+\xi^2\right)} \left(\left(1+\xi\alpha\right) \mathbf{m} \times \left(\mathbf{m} \times (\mathbf{J} \cdot \nabla)\mathbf{m} \right) + \left(\xi - \alpha\right) \mathbf{m} \times (\mathbf{J} \cdot \nabla)\mathbf{m} \right) \tag{24}$$

where ξ is the degree of non-adiabaticity.

The effective field corresponding to a Zhang-Li spin-transfer torque is given by

$$\mathbf{H}_{\mathrm{ST}} = -\frac{\mu_B}{2e\gamma_0 M_S\left(1+\xi^2\right)} \left(\left(\mathbf{m} \times (\mathbf{J} \cdot \nabla)\mathbf{m} \right) + \xi(\mathbf{J} \cdot \nabla)\mathbf{m} \right) \tag{25}$$

The energy density of a spin torque is given by

$$f_{\mathrm{ST}} = -\mu_0 M_S \mathbf{H}_{\mathrm{ST}} \cdot \mathbf{m} \tag{26}$$

2.9 Thermal fluctuation

The thermal fluctuation field is given by

$$\mathbf{H}_{\mathrm{therm}} = \boldsymbol{\eta}\sqrt{\frac{2\alpha k_B T}{\mu_0 M_S \gamma_0 \Delta V \Delta t}} \tag{27}$$

where $k_B = 1.38064853 \times 10^{-23} \mathrm{J \cdot K^{-1}}$ is the Boltzmann constant, T is the Kelvin temperature, $\Delta V = \Delta l_1 \times \Delta l_2 \times \Delta l_3$ is the volume of a grid, and $\boldsymbol{\eta}$ is a random vector with three independent

12

components η_1, η_2, and η_3 all obeying standard normal distribution. Values of these three components are independent at each evolution step.

3 Input files

Users need to prepare one through five files as input:

3.1 *parameterFormatted.in* or alternatively *parameter.in*

Declares the size of the system, the type of properties considered, properties of each phase, and external fields applied. Users shall provide either *parameterFormatted.in* (fixed-format version) or *parameter.in* (free-format version). If both files are provided, only *parameter.in* will be adopted.

The format is as follows:

Table 3.1 Format of the input file *parameterFormatted.in*

Data in the file			Explanation
l_1	l_2	l_3	System real size along x_1, x_2, and x_3 directions (nm)
n_1	n_2	n_3	Total number of simulation grids along x_1, x_2, and x_3 directions
n_s	n_f		See Section 2.1
C_{Island}			See Section 2.1
n_{i1}	n_{i2}	n_{i3}	See Section 2.1
C_{Grain}			Choice of crystalline grain structure: 0-Euler angles φ, θ, and ψ (°) array read from file *eulerAng.in*; 1-single crystal with specified Euler angles
$φ_C$	$θ_C$	$ψ_C$	(For C_{Grain}=1) Euler angles φ, θ, and ψ (°) of the single crystal orientation
M_S	$γ$	$α$	M_S – saturation magnetization (A/m); $γ$ – electron gyromagnetic ratio (m/(A.s)); $α$ – damping constant (unitless)
Fl_{Anis}			Flag of whether to consider magnetocrystalline anisotropy
C_{Anis}			(For Fl_{Anis}=true) choice of type of magnetocrystalline anisotropy: 1-cubic; 2-uniaxial
K_1	K_2	K_3	(For Fl_{Anis}=true and C_{Anis}=1) K_1, K_2, K_3 – cubic magnetocrystalline anisotropy coefficient **K** (J/m^3); (For Fl_{Anis}=true and C_{Anis}=2) K_1, K_2 – uniaxial magnetocrystalline anisotropy coefficient **K** (J/m^3)
Fl_{Stray}			Flag of whether to consider stray field
C_{MBC}			(For Fl_{Stray}=true) choice of type of magnetostatic boundary condition: 1-finite-size; 2-periodic; 3-finite-size in-plane, periodic out-of-plane
N_{D11}	N_{D22}	N_{D33}	(For Fl_{Stray}=true and C_{MBC}=2) demagnetizing factor **N$_D$** (unitless)
N_{D23}	N_{D13}	N_{D12}	

C_{Hext}			Choice of external magnetic field: 0-an array of field sequence read from file *hExt.in* with possible linear interpolations; 1-DC and AC components defined in the following three lines, i.e., $\mathbf{H}_{ext} = \mathbf{H}_{DC} + \mathbf{H}_{AC}\sin(2\pi f_{AC} \cdot t)$
H_{DC1}	H_{DC2}	H_{DC3}	(For C_{Hext}=1) DC component of external magnetic field $\mathbf{H}_{DC}$ (A/m)
H_{AC1}	H_{AC2}	H_{AC3}	(For C_{Hext}=1) magnitude of AC component of external magnetic field $\mathbf{H}_{AC}$ (A/m)
f_{AC}			(For C_{Hext}=1) frequency of AC component of external magnetic field (Hz)
Fl_{Elas}			Flag of whether to consider magnetoelastic effect
λ_{100}	λ_{111}		(For Fl_{Elas}=true) saturation magnetostriction λ (unitless)
$c_{1'1'}$	$c_{1'2'}$	$c_{4'4'}$	(For Fl_{Elas}=true) elastic stiffness **c** of the magnet in Voigt notation (Pa)
$c_{s1'1'}$	$c_{s1'2'}$	$c_{s4'4'}$	(For film or island, and Fl_{Elas}=true) elastic stiffness $\mathbf{c}_s$ of the substrate in Voigt notation (Pa)
C_{EBC}			(For bulk and Fl_{Elas}=true) choice of type of bulk elastic boundary condition: 1-applied external strain; 2-applied external stress
C_{Sext}			(For Fl_{Elas}=true) choice of external strain/stress: 0-an array of strain/stress sequence read from file *sExt.in* with possible linear interpolations; 2-static stress/strain defined in the following two lines
ε_{ext11} or σ_{ext11}	ε_{ext22} or σ_{ext22}	ε_{ext12} or σ_{ext12}	(For film or island, F_{Elas}=true, and C_{Sext}=1) in-plane substrate strain $\boldsymbol{\varepsilon}_{ext}$; (For bulk, Fl_{Elas}=true, C_{EBC}=1, and C_{Sext}=1) in-plane components of applied strains $\boldsymbol{\varepsilon}_{ext}$ (unitless); (For bulk, Fl_{Elas}=true, C_{EBC}=2, and C_{Sext}=1) in-plane components of applied stress $\boldsymbol{\sigma}_{ext}$ (Pa)
ε_{ext33} or σ_{ext33}	ε_{ext13} or σ_{ext13}	ε_{ext23} or σ_{ext23}	(For bulk, Fl_{Elas}=true, C_{EBC}=1, and C_{Sext}=1) out-of-plane components of applied strains $\boldsymbol{\varepsilon}_{ext}$ (unitless); (For bulk, Fl_{Elas}=true, C_{EBC}=2, and C_{Sext}=1) out-of-plane components of applied stress $\boldsymbol{\sigma}_{ext}$ (Pa)
n_{Recurs}	Δe		(For Fl_{Elas}=true, and with inhomogeneous elastic stiffness in the system) n_{Recurs} – maximum number of recursion loops for elastic solver; (For Fl_{Elas}=true, and with inhomogeneous elastic stiffness in the system) Δe – maximum error for elastic solver
Fl_{InStra}			(For Fl_{Elas}=true, and with inhomogeneous elastic stiffness in the system) flag of whether to input the solved strain distribution of the initial evolution step
A			Magnetic exchange energy coefficient (J/m)
Fl_{DMI}			Flag of whether to consider Dzyaloshinskii-Moriya interaction (DMI)
D			(For Fl_{DMI}=true) continuous effective DMI constant
F_{ST}			Flag of whether to consider spin torque
C_{ST}			(For Fl_{ST}=true) type of spin torque: 1-spin-orbit torque 2-Slonczewski spin-transfer torque 3-Zhang-Li spin-transfer-torque
θ_{SH}			(For Fl_{ST}=true, and C_{ST}=1) spin Hall angle in a spin-orbit torque
J			(For Fl_{ST}=true, and C_{ST}=1 or 2) J – spin-polarized electric current density direction (A/m^2)
m_{P1}	m_{P2}	m_{P3}	(For Fl_{ST}=true, and C_{ST}=1 or 2) normalized magnetization $\mathbf{m}_P$ in the fixed layer in a spin torque structure (unitless)
η_{SP}			(For Fl_{ST}=true, and C_{ST}=2) spin polarization constant in a Slonczewski spin-transfer torque
ξ_{STT}			(For Fl_{ST}=true, and C_{ST}=3) degree of non-adiabaticity in a Zhang-Li spin-transfer torque
J_1	J_2	J_3	(For Fl_{ST}=true, and C_{ST}=3) J_1, J_2, J_3 – spin-polarized electric current density **J** (A/m^2)
Fl_{Therm}			Flag of whether to consider thermal fluctuation field
T			(For Fl_{Therm}=true) temperature (K)

C_{LLG}			Type of LLG numerical solver: 1-implicit Gauss-Seidel using Fourier spectral 2-explicit RK4	
Δt			Time per evolution step (s)	
k_{t0}	k_{tMax}		k_{t0} – number of the starting evolution step; k_{tMax} – number of the finishing evolution step	
k_{tTable}	k_{tDist}		k_{tTable} – output step interval for data table; k_{tDist} – output step interval for spatial distribution	
$C_{InitialM}$			Choice of initial magnetization distribution: 0-an array of magnetization distribution read from file *Magnt.in*; 1-random orientation; 2-specified uniform orientation; 3-specified vortex domain	
a_1	a_2	a_3	(For $C_{InitialM}$=2) axis of **a** uniform orientation of the initial magnetization; (For $C_{InitialM}$=3) axis of **a** vortex of the initial magnetization	
Fl_{OutH}	Fl_{OutE}		Fl_{OutH} – flag of whether to output distribution of effective fields Fl_{OutE} – flag of whether to output distribution of energy densities	
Fl_{OutS}			(For Fl_{Elas}=true) flag of whether to output distribution of eigenstrain, strain, and stress	

Table 3.1.2 Format of the input file *parameter.in*

Module	Identifier in the file	Data following the identifier in the file						Default value
Size	REALDIM	l_1	l_2	l_3				30
	SYSDIM	n_1	n_2	n_3				10
	SUBTHICK	n_s						0
	FILMTHICK	n_f						0
	ISLANDTHICK	n_{i3}						0
	CHOICEINISLAND	C_{Island}						1
	ISLANDLENGTH	n_{i1}	n_{i2}					0
Crystal Orientation	CHOICEINGRAIN	C_{Grain}						1
	EULERANGLE	φ_C	θ_C	ψ_C				0
Spin	SATURATION	M_S						5×10^5
	GYROMAG	γ						2.211×10^6
	DAMPING	α						0.5
Anisotropy	FLAGANI	Fl_{Anis}						false
	CHOICEANI	C_{Anis}						1
	ANISOTROPY	K_1	K_2	K_3				0
Stray	FLAGSTRAY	Fl_{Stray}						true
	CHOICEMSTATBC	C_{MBC}						false
	DEMAGFACTOR	N_{D11}	N_{D22}	N_{D33}	N_{D23}	N_{D13}	N_{D12}	0
External Field	CHOICEINFIELD	C_{Hext}						1
	DCFIELD	H_{DC1}	H_{DC2}	H_{DC3}				0
	ACFIELD	H_{AC1}	H_{AC2}	H_{AC3}				0
	FIELDFREQ	f_{AC}						0
Elastic	FLAGELASTIC	Fl_{Elas}						false
	MAGSTRICTION	λ_{100}	λ_{111}					0
	STIFFNESS	$c_{1'1'}$	$c_{1'2'}$	$c_{4'4'}$				$c_{1'1'}$=1×10^{11} $c_{1'2'}$=4×10^{10} $c_{4'4'}$=3×10^{10}
	SUBSTIFFNESS	$c_{s1'1'}$	$c_{s1'2'}$	$c_{s4'4'}$				$c_{s1'1'}$=1×10^{11} $c_{s1'2'}$=4×10^{10} $c_{s4'4'}$=3×10^{10}
	CHOICEELABC	C_{EBC}						1
	CHOICEINELAAPP	C_{Sext}						1
	ELAAPPINPLANE	ε_{ext11} or	ε_{ext22} or	ε_{ext12} or				0

		σ_{ext11}	σ_{ext22}	σ_{ext12}					
	ELAAPPOUTPLANE	ε_{ext33} or σ_{ext33}	ε_{ext13} or σ_{ext13}	ε_{ext23} or σ_{ext23}					0
	ELARECURS	n_{Recurs}							1000
	ELATOLER	Δe							1×10^{-4}
	FLAGINSTRAIN	Fl_{InStra}							false
Exchange	EXCHANGE	A							1×10^{-11}
DMI	FLAGDMI	Fl_{DMI}							false
	DMI	D							0
Spin Torque	FLAGSPINTORQ	F_{ST}							false
	CHOICESPINTORQ	C_{ST}							1
	SPINHALLANGLE	θ_{SH}							0
	ELECCURR	J							0
	FIXEDMAG	m_{P1}	m_{P2}	m_{P3}					0
	SPINPOLAR	η_{SP}							0
	NONADIAB	ξ_{STT}							0
	ELECCURRZL	J_1	J_2	J_3					0
Thermal	FLAGTHERMAL	Fl_{Therm}							false
	TEMPERATURE	T							298
Time	CHOICELLG	C_{LLG}							1
	TIMESTEP	Δt							1×10^{-13}
	NTSTART	k_{t0}							0
	NTMAX	k_{tMax}							10000
	NTOUTTABLE	k_{tTable}							100
	NTOUTDIST	k_{tDist}							1000
	CHOICEINITMAG	$C_{InitialM}$							1
	INITMAG	a_1	a_2	a_3					$a_1=a_2=0, a_3=1$
Output	FLAGOUTEFFFIELD	Fl_{OutH}							false
	FLAGOUTENERGY	Fl_{OutE}							false
	FLAGOUTELASTIC	Fl_{OutS}							false

Explanations of variables in Table 3.1.2 are the same as in Table 3.1.1, and are hence omitted.

3.2 *islandShape.in* (optional)

Contains an array $o_{m2d}\left(x_1, x_2\right)$ describing the 2-d in-plane shape of a magnetic island. This file is used only in an island-on-substrate or a finite-size magnet system with $C_{Island}=0$, as defined in the file *parameterFormatted.in*.

The format is as follows:

Table 3.2 Format of the input file *islndShape.in*

Data in the file			Explanation
1	1	$o_{m2d}(1, 1)$	If $o_{m2d}(1, 1)=1$, grid points $(1, 1, k)$ where k is within the thickness of the island are considered within the magnetic island, i.e., $o_m(1, 1, k)=1$. If $o_{m2d}(1, 1)=0$, grid points $(1, 1, k)$ where k is within the thickness of the island are considered vacuum, i.e., $o_m(1, 1, k)=0$.
⋮	⋮	⋮	
1	n_2	$o_{m2d}(1, n_2)$	
⋮	⋮	⋮	
n_1	n_2	$o_{m2d}(n_1, n_2)$	

3.3 *eulerAng.in* (optional)

Contains an array of the distribution of the Euler angles $\varphi(\mathbf{x})$, $\theta(\mathbf{x})$, and $\psi(\mathbf{x})$ of grains in polycrystals, arranged in a row-major order. This file is used only with $C_{Grain}=0$, as defined in the file *parameterFormatted.in*.

The format is as follows:

Table 3.3 Format of the input file *eulerAng.in*

Data in the file						Explanation
n_1	n_2	n_3				Total number of simulation grids in each direction
1	1	1	$\varphi(1, 1, 1)$	$\theta(1, 1, 1)$	$\psi(1, 1, 1)$	φ, θ, ψ – Euler angles of the grain containing the grid point (1, 1, 1) (°)
		⋮				⋮
1	1	n_3	$\varphi(1, 1, n_3)$	$\theta(1, 1, n_3)$	$\psi(1, 1, n_3)$	⋮
		⋮				⋮
1	n_2	n_3	$\varphi(1, n_2, n_3)$	$\theta(1, n_2, n_3)$	$\psi(1, n_2, n_3)$	⋮
		⋮				⋮
n_1	n_2	n_3	$\varphi(n_1, n_2, n_3)$	$\theta(n_1, n_2, n_3)$	$\psi(n_1, n_2, n_3)$	⋮

3.4 *hExt.in* (optional)

Contains an array of the external magnetic field sequence $\mathbf{H}_{ext}(k_t)$. This file is used only with $C_{Hext}=0$, as defined in the file *parameterFormatted.in*.

The format is as follows:

Table 3.4 Format of the input file *hExt.in*

Data in the file				Explanation
n				Total number of following lines in this file
k_{t1}	$H_{ext1}(k_{t1})$	$H_{ext2}(k_{t1})$	$H_{ext3}(k_{t1})$	$\mathbf{H}_{ext}(k_{t1})$ – external magnetic field $\mathbf{H}_{ext}$ at the k_{t1}-th evolution step (A/m)
k_{t2}	$H_{ext1}(k_{t2})$	$H_{ext2}(k_{t2})$	$H_{ext3}(k_{t2})$	⋮
⋮	⋮	⋮	⋮	⋮
k_{tn}	$H_{ext1}(k_{tn})$	$H_{ext2}(k_{tn})$	$H_{ext3}(k_{tn})$	⋮

In obtaining $\mathbf{H}_{ext}(k_t)$ at all evolution steps k_t, the program considers linear interpolations of $\mathbf{H}_{ext}(k_t)$ between adjacent evolution steps k_t provided in this file.

3.5 *sExt.in* (optional)

Contains an array of the applied external strain sequence $\boldsymbol{\varepsilon}_{ext}(k_t)$, or stress sequence $\boldsymbol{\sigma}_{ext}(k_t)$. This file is used only with Fl$_{Elas}$=true and C$_{Sext}$=0, as defined in the file *parameterFormatted.in*. For a bulk system, all 6 components of applied strain/stress needs to be provided in the file, while for a thin film or an island system, only 3 in-plane substrate strain components shall be provided.

The format is as follows:

Table 3.5.1 Format of the input file *sExt.in* for a bulk system

Data in the file						Explanation
n						Total number of following lines in this file
k_{t1}	$\varepsilon_{ext11}(k_{t1})$ or $\sigma_{ext11}(k_{t1})$	$\varepsilon_{ext22}(k_{t1})$ or $\sigma_{ext22}(k_{t1})$	$\varepsilon_{ext33}(k_{t1})$ or $\sigma_{ext33}(k_{t1})$	$\varepsilon_{ext23}(k_{t1})$ or $\sigma_{ext23}(k_{t1})$	$\varepsilon_{ext13}(k_{t1})$ or $\sigma_{ext13}(k_{t1})$	$\varepsilon_{ext12}(k_{t1})$ or $\sigma_{ext12}(k_{t1})$	(For C$_{EBC}$=1) $\boldsymbol{\varepsilon}_{ext}(k_{t1})$ – applied strain $\boldsymbol{\varepsilon}_{ext}$ at the k_{t1}-th evolution step (For C$_{EBC}$=2) $\boldsymbol{\sigma}_{ext}(k_{t1})$ – applied stress $\boldsymbol{\sigma}_{ext}$ at the k_{t1}-th evolution step (Pa)
k_{t2}	$\varepsilon_{ext11}(k_{t2})$ or $\sigma_{ext11}(k_{t2})$	$\varepsilon_{ext22}(k_{t2})$ or $\sigma_{ext22}(k_{t2})$	$\varepsilon_{ext33}(k_{t2})$ or $\sigma_{ext33}(k_{t2})$	$\varepsilon_{ext23}(k_{t2})$ or $\sigma_{ext23}(k_{t2})$	$\varepsilon_{ext13}(k_{t2})$ or $\sigma_{ext13}(k_{t2})$	$\varepsilon_{ext12}(k_{t2})$ or $\sigma_{ext12}(k_{t2})$	$\vdots$
$\vdots$				$\vdots$	$\vdots$	$\vdots$	$\vdots$
k_{tn}	$\varepsilon_{ext11}(k_{tn})$ or $\sigma_{ext11}(k_{tn})$	$\varepsilon_{ext22}(k_{tn})$ or $\sigma_{ext22}(k_{tn})$	$\varepsilon_{ext33}(k_{tn})$ or $\sigma_{ext33}(k_{tn})$	$\varepsilon_{ext23}(k_{tn})$ or $\sigma_{ext23}(k_{tn})$	$\varepsilon_{ext13}(k_{tn})$ or $\sigma_{ext13}(k_{tn})$	$\varepsilon_{ext12}(k_{tn})$ or $\sigma_{ext12}(k_{tn})$	$\vdots$

Table 3.5.2 Format of the input file *sExt.in* for a thin film or an island system

Data in the file			Explanation
n			Total number of following lines in this file
k_{t1}	$\varepsilon_{ext11}(k_{t1})$	$\varepsilon_{ext22}(k_{t1})$	$\varepsilon_{ext12}(k_{t1})$	$\varepsilon_{ext11}(k_{t1})$, $\varepsilon_{ext22}(k_{t1})$, and $\varepsilon_{ext12}(k_{t1})$ – components of in-plane substrate strain $\boldsymbol{\varepsilon}_{ext}$ at the k_{t1}-th evolution step
k_{t2}	$\varepsilon_{ext11}(k_{t2})$	$\varepsilon_{ext22}(k_{t2})$	$\varepsilon_{ext12}(k_{t2})$	$\vdots$
$\vdots$	$\vdots$	$\vdots$	$\vdots$	$\vdots$
k_{tn}	$\varepsilon_{ext11}(k_{tn})$	$\varepsilon_{ext22}(k_{tn})$	$\varepsilon_{ext12}(k_{tn})$	$\vdots$

In obtaining $\boldsymbol{\varepsilon}_{ext}(k_t)$ or $\boldsymbol{\sigma}_{ext}(k_t)$ at all evolution steps k_t, the program considers linear interpolations of $\boldsymbol{\varepsilon}_{ext}(k_t)$ or $\boldsymbol{\sigma}_{ext}(k_t)$ between adjacent evolution steps k_t provided in this file.

3.6 *strain.in* (optional)

Contains an array of the distribution of initial strain $\boldsymbol{\varepsilon}(\mathbf{x}, k_{t0})$, arranged in a row-major order. This file is used only with Fl$_{Elas}$=true and Fl$_{InStra}$=true, as defined in the file *parameterFormatted.in*, in a system with inhomogeneous elastic stiffness.

The format is as follows:

Table 3.6 Format of the input file *strain.in*

Data in the file								Explanation
n_1	n_2	n_3						Total number of simulation grids in each direction

1	1	1	$\varepsilon_{11}(1,1,1)$	$\varepsilon_{22}(1,1,1)$	$\varepsilon_{33}(1,1,1)$	$\varepsilon_{23}(1,1,1)$	$\varepsilon_{13}(1,1,1)$	$\varepsilon_{12}(1,1,1)$	$\boldsymbol{\varepsilon}$ – Normalized initial strain $\boldsymbol{\varepsilon}$ at grid point (1,1,1)
						⋮			⋮
1	1	n_3	$\varepsilon_{11}(1,1,n_3)$	$\varepsilon_{22}(1,1,n_3)$	$\varepsilon_{33}(1,1,n_3)$	$\varepsilon_{23}(1,1,n_3)$	$\varepsilon_{13}(1,1,n_3)$	$\varepsilon_{12}(1,1,n_3)$	⋮
						⋮			⋮
1	n_2	n_3	$\varepsilon_{11}(1,n_2,n_3)$	$\varepsilon_{22}(1,n_2,n_3)$	$\varepsilon_{33}(1,n_2,n_3)$	$\varepsilon_{23}(1,n_2,n_3)$	$\varepsilon_{13}(1,n_2,n_3)$	$\varepsilon_{12}(1,n_2,n_3)$	⋮
						⋮			⋮
n_1	n_2	n_3	$\varepsilon_{11}(n_1,n_2,n_3)$	$\varepsilon_{22}(n_1,n_2,n_3)$	$\varepsilon_{33}(n_1,n_2,n_3)$	$\varepsilon_{23}(n_1,n_2,n_3)$	$\varepsilon_{13}(n_1,n_2,n_3)$	$\varepsilon_{12}(n_1,n_2,n_3)$	⋮

3.7 *magnt.in* (optional)

Contains an array of the distribution of initial magnetization $\mathbf{m}(\mathbf{x}, k_{t0})$, arranged in a row-major order. This file is used only with C$_{InitialM}$=0, as defined in the file *parameterFormatted.in*.

The format is as follows:

Table 3.7 Format of the input file *magnt.in*

Data in the file						Explanation
n_1	n_2	n_3				Total number of simulation grids in each direction
1	1	1	$m_1(1, 1, 1)$	$m_2(1, 1, 1)$	$m_3(1, 1, 1)$	$\mathbf{m}$ – Normalized initial magnetization $\mathbf{m}$ at grid point (1,1,1) (unitless)
				⋮		⋮
1	1	n_3	$m_1(1, 1, n_3)$	$m_2(1, 1, n_3)$	$m_3(1, 1, n_3)$	⋮
				⋮		⋮
1	n_2	n_3	$m_1(1, n_2, n_3)$	$m_2(1, n_2, n_3)$	$m_3(1, n_2, n_3)$	⋮
				⋮		⋮
n_1	n_2	n_3	$m_1(n_1, n_2, n_3)$	$m_2(n_1, n_2, n_3)$	$m_3(n_1, n_2, n_3)$	⋮

4 Ouput files

4.1 Files generated before doing evolution

oMag.00000000.dat

Contains an array of $o_m(\mathbf{x})$ (unitless), arranged in a row-major order. The data follow a similar format with those in *magnt.in*. The file is generated before simulating evolution steps.

cGlob.00000000.dat (optional)

Contains an array of $c_{11}(\mathbf{x})$, $c_{22}(\mathbf{x})$, and $c_{44}(\mathbf{x})$ (Pa) in Voigt notation, arranged in a row-major order. The data follow a similar format with those in *magnt.in*. The file is generated before simulating evolution steps and only under Fl$_{Elas}$=true.

hExt.dat

Contains an array of the external magnetic field sequence $H_{ext1}(k_t)$, $H_{ext2}(k_t)$, and $H_{ext3}(k_t)$ (A/m) at all evolution steps. The data follow a similar format with those in *hExt.in*. The file is generated before simulating evolution steps.

sExt.dat

Contains an array of the sequence of applied strain $\varepsilon_{ext11}(k_t)$, $\varepsilon_{ext22}(k_t)$, $\varepsilon_{ext33}(k_t)$, $\varepsilon_{ext23}(k_t)$, $\varepsilon_{ext13}(k_t)$, $\varepsilon_{ext12}(k_t)$, applied stress $\sigma_{ext11}(k_t)$, $\sigma_{ext22}(k_t)$, $\sigma_{ext33}(k_t)$, $\sigma_{ext23}(k_t)$, $\sigma_{ext13}(k_t)$ $\sigma_{ext12}(k_t)$ (Pa), or substrate strain $\varepsilon_{ext11}(k_t)$, $\varepsilon_{ext22}(k_t)$, $\varepsilon_{ext12}(k_t)$, at all evolution steps. The data follow a similar format with those in *sExt.in*. The file is generated before simulating evolution steps.

4.2 Files generated during evolution steps

avMagntz.dat

Contains an array of average values of the normalized magnetization $\overline{m_1}(k_t)$, $\overline{m_2}(k_t)$, and $\overline{m_3}(k_t)$ (unitless) inside the magnet at every k$_{tTable}$ evolution steps. The data follow a similar format with those in *hExt.in*. The file is updated every k$_{tTable}$ steps.

avHEff.dat

Contains an array of average values of the effective fields $H_{ext1}(k_t)$, $H_{ext2}(k_t)$, $H_{ext3}(k_t)$, $\overline{H_{eff1}}(k_t)$, $\overline{H_{eff2}}(k_t)$, $\overline{H_{eff3}}(k_t)$, $\overline{H_{stray1}}(k_t)$, $\overline{H_{stray2}}(k_t)$, $\overline{H_{stray3}}(k_t)$, $\overline{H_{anis1}}(k_t)$, $\overline{H_{anis2}}(k_t)$, $\overline{H_{anis3}}(k_t)$, $\overline{H_{elas1}}(k_t)$, $\overline{H_{elas2}}(k_t)$, $\overline{H_{elas3}}(k_t)$, $\overline{H_{ST1}}(k_t)$, $\overline{H_{ST2}}(k_t)$, $\overline{H_{ST3}}(k_t)$, $\overline{H_{therm1}}(k_t)$, $\overline{H_{therm2}}(k_t)$, and $\overline{H_{therm3}}(k_t)$ (A/m) inside the magnet at every k$_{tTable}$ evolution steps. The data follow a similar format with those in *hExt.in*. The file is updated every k$_{tTable}$ steps.

avEnergy.dat

Contains an array of average values of the energy densities $\overline{f}(k_t)$, $\overline{f_{ext}}(k_t)$, $\overline{f_{stray}}(k_t)$, $\overline{f_{anis}}(k_t)$, $\overline{f_{elas}}(k_t)$, $\overline{f_{exch}}(k_t)$, $\overline{f_{DMI}}(k_t)$, and $\overline{f_{ST}}(k_t)$ (J/m^3) inside the magnet at every k$_{tTable}$ evolution steps. The data follow a similar format with those in *hExt.in*. The file is updated every k$_{tTable}$ steps.

avStrain.dat (optional)

Contains an array of average values of the strain and eigenstrain $\overline{\varepsilon_{11}}(k_t)$, $\overline{\varepsilon_{22}}(k_t)$, $\overline{\varepsilon_{33}}(k_t)$, $\overline{\varepsilon_{23}}(k_t)$, $\overline{\varepsilon_{13}}(k_t)$, $\overline{\varepsilon_{12}}(k_t)$, $\overline{\varepsilon_{11}^0}(k_t)$, $\overline{\varepsilon_{22}^0}(k_t)$, $\overline{\varepsilon_{33}^0}(k_t)$, $\overline{\varepsilon_{23}^0}(k_t)$, $\overline{\varepsilon_{13}^0}(k_t)$, and $\overline{\varepsilon_{12}^0}(k_t)$ (unitless) inside the magnet at every k_{tTable} evolution steps. The data follow a similar format with those in *hExt.in*. The file is updated every k_{tTable} steps, and only under Fl_{Elas}=true.

avStress.dat (optional)

Contains an array of average values of the stress $\overline{\sigma_{11}}(k_t)$, $\overline{\sigma_{22}}(k_t)$, $\overline{\sigma_{33}}(k_t)$, $\overline{\sigma_{23}}(k_t)$, $\overline{\sigma_{13}}(k_t)$, and $\overline{\sigma_{12}}(k_t)$ (Pa) inside the magnet at every k_{tTable} evolution steps. The data follow a similar format with those in *hExt.in*. The file is updated every k_{tTable} steps, and only under Fl_{Elas}=true.

*magnt.**.dat*

Contains an array of $m_1(\mathbf{x})$, $m_2(\mathbf{x})$, and $m_3(\mathbf{x})$ (unitless) at a certain evolution step, arranged in a row-major order, where ** represents the 8-digit evolution step number. The data follow a similar format with those in *magnt.in*. A file is generated every k_{tDist} steps.

*hEff.**.dat* (optional)

Contains an array of $H'_{eff1}(\mathbf{x})$, $H'_{eff2}(\mathbf{x})$, and $H'_{eff3}(\mathbf{x})$ (A/m) at a certain evolution step, arranged in a row-major order, where ** represents the 8-digit evolution step number. The data follow a similar format with those in *magnt.in*. A file is generated every k_{tDist} steps and only under Fl_{OutH}=true.

*hStra.**.dat* (optional)

Contains an array of $H_{stray1}(\mathbf{x})$, $H_{stray2}(\mathbf{x})$, and $H_{stray3}(\mathbf{x})$ (A/m) at a certain evolution step, arranged in a row-major order, where ** represents the 8-digit evolution step number. The data follow a similar format with those in *magnt.in*. A file is generated every k_{tDist} steps and only under Fl_{OutH}=true and Fl_{Stray}=true.

*hAnis.**.dat* (optional)

Contains an array of $H_{anis1}(\mathbf{x})$, $H_{anis2}(\mathbf{x})$, and $H_{anis3}(\mathbf{x})$ (A/m) at a certain evolution step, arranged in a row-major order, where ** represents the 8-digit evolution step number. The data follow a similar format with those in *magnt.in*. A file is generated every k_{tDist} steps and only under Fl_{OutH}=true and Fl_{Anis}=true.

*hElas.**.dat* (optional)

Contains an array of H_{elas1}, H_{elas2}, and H_{elas3} (A/m) at a certain evolution step, arranged in a row-major order, where ** represents the 8-digit evolution step number. The data follow a similar format with those in *magnt.in*. A file is generated every k_{tDist} steps and only under Fl_{OutH}=true and Fl_{Elas}=true.

*hST.**.dat* (optional)

Contains an array of $H_{\text{ST1}}(\mathbf{x})$, $H_{\text{ST2}}(\mathbf{x})$, and $H_{\text{ST3}}(\mathbf{x})$ (A/m) at a certain evolution step, arranged in a row-major order, where ** represents the 8-digit evolution step number. The data follow a similar format with those in *magnt.in*. A file is generated every k_{tDist} steps and only under Fl_{OutH}=true and Fl_{ST}=true.

*hTher.**.dat* (optional)

Contains an array of $H_{\text{therm1}}(\mathbf{x})$, $H_{\text{therm2}}(\mathbf{x})$, and $H_{\text{therm3}}(\mathbf{x})$ (A/m) at a certain evolution step, arranged in a row-major order, where ** represents the 8-digit evolution step number. The data follow a similar format with those in *magnt.in*. A file is generated every k_{tDist} steps and only under Fl_{OutH}=true and Fl_{Therm}=true.

*eigStn.**.dat* (optional)

Contains an array of $\varepsilon_{11}^{0}(\mathbf{x})$, $\varepsilon_{22}^{0}(\mathbf{x})$, $\varepsilon_{33}^{0}(\mathbf{x})$, $\varepsilon_{23}^{0}(\mathbf{x})$, $\varepsilon_{13}^{0}(\mathbf{x})$, and $\varepsilon_{12}^{0}(\mathbf{x})$ (unitless) at a certain evolution step, arranged in a row-major order, where ** represents the 8-digit evolution step number. The data follow a similar format with those in *magnt.in*. A file is generated every k_{tDist} steps and only under Fl_{OutS}=true and Fl_{Elas}=true.

*strain.**.dat* (optional)

Contains an array of $\varepsilon_{11}(\mathbf{x})$, $\varepsilon_{22}(\mathbf{x})$, $\varepsilon_{33}(\mathbf{x})$, $\varepsilon_{23}(\mathbf{x})$, $\varepsilon_{13}(\mathbf{x})$, and $\varepsilon_{12}(\mathbf{x})$ (unitless) at a certain evolution step, arranged in a row-major order, where ** represents the 8-digit evolution step number. The data follow a similar format with those in *magnt.in*. A file is generated every k_{tDist} steps and only under Fl_{OutS}=true and Fl_{Elas}=true.

*stress.**.dat* (optional)

Contains an array of $\sigma_{11}(\mathbf{x})$, $\sigma_{22}(\mathbf{x})$, $\sigma_{33}(\mathbf{x})$, $\sigma_{23}(\mathbf{x})$, $\sigma_{13}(\mathbf{x})$, and $\sigma_{12}(\mathbf{x})$ (Pa) at a certain evolution step, arranged in a row-major order, where ** represents the 8-digit evolution step number. The data follow a similar format with those in *magnt.in*. A file is generated every k_{tDist} steps and only under Fl_{OutS}=true and Fl_{Elas}=true.

5 Examples

5.1 μMag Standard Problem #1

μMag Standard Problem #1 considers the M-H hysteresis loop of a 1μm × 2μm × 20nm permalloy rectangle with the following material parameters:
$M_S = 8 \times 10^5$ A/m

A = 1.3×10^{-11} J/m
K_1 = 5×10^2 J/m^3 (Uniaxial anisotropy)
on applying a magnetic field approximately parallel to the long and short axis of the magnet.

The solution using μ-Pro® Mag is presented in the following figures. Since submitted solutions on the μMag website don't agree with each other, the correctness of the solution couldn't be tested.
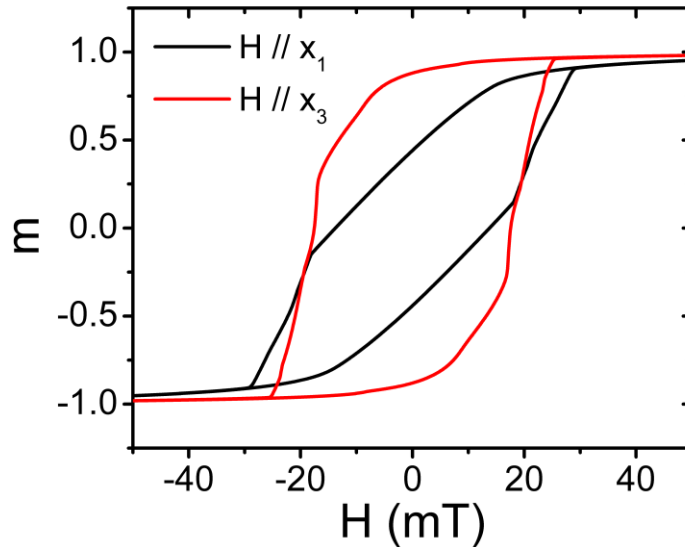

Figure 5.1.1 M-H hysteresis loop on applying a magnetic field parallel to the long axis (H // x_1) and the short axis (H // x_3), respectively.
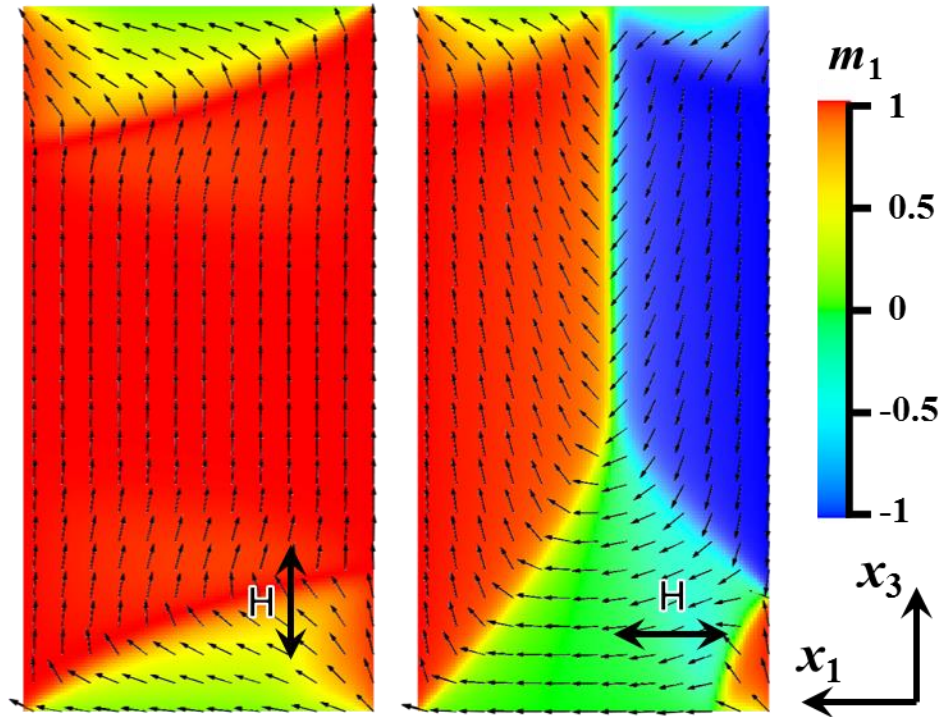
Figure 5.1.2 Remnant magnetic domain configuration on applying a magnetic field parallel to the long axis (left) and the short axis (right), respectively.

5.2 μMag Standard Problem #2

μMag Standard Problem #2 considers the scaling effect on remnant magnetization m_R and coercive field H_C of a magnet with the size of $5d \times d \times 0.1d$, i.e., m_R and H_C as a function of d/l_{ex}, with exchange length $l_{ex} = sqrt(A/K_m)$, where K_m is the magnetostatic energy density defined as $K_m = \frac{1}{2}\mu_0 M_S^2$. The magnetic field is applied in the [1,1,1] direction.

The solution using μ-Pro® Mag is presented in the following figures. The remnant magnetization agrees well with Streibl and Donahue's solution submitted to the μMag group[14].
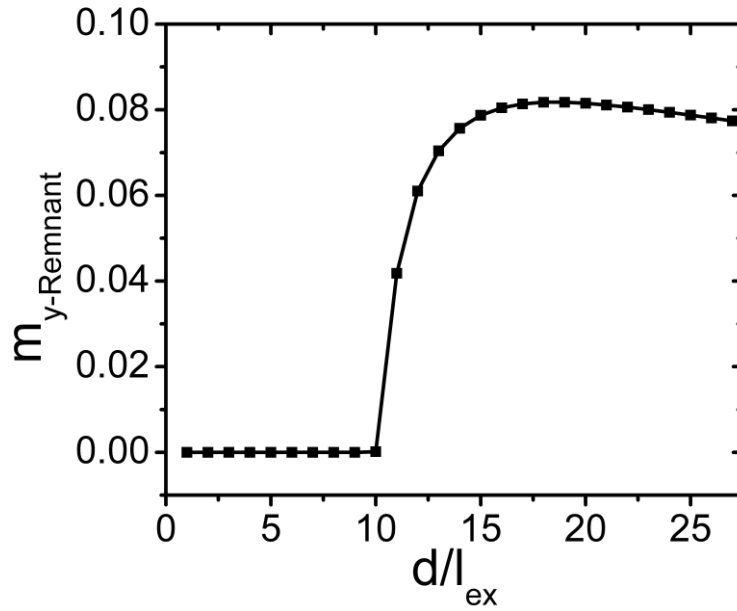
Figure 5.2.1 Remnant magnetization m_{x-R} as a function of d/l_{ex}.
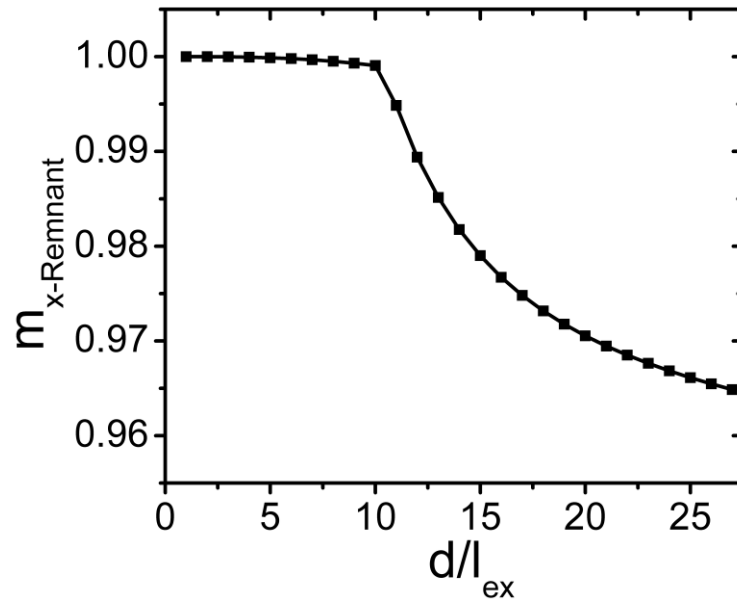
Figure 5.2.2 Remnant magnetization m_{y-R} as a function of d/l_{ex}.

25
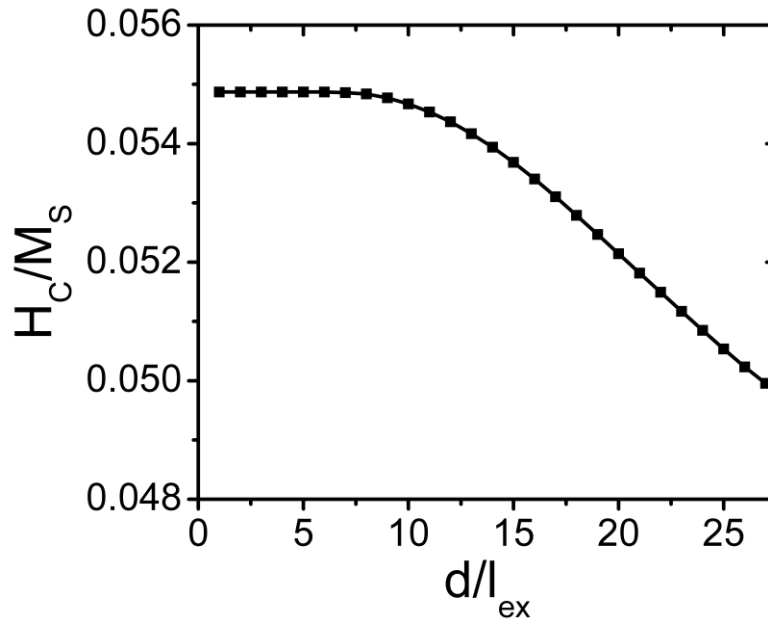
Figure 5.2.3 Coercive field H_C as a function of d/l_{ex}.

5.3 µMag Standard Problem #3

µMag Standard Problem #3 models the transition of the stable magnetic domain structure from a flower state to a vortex state on increasing size of a magnet. A cubic magnet with edge length L expressed in units of exchange length $l_{ex} = \text{sqrt}(A/K_m)$, where K_m is the magnetostatic energy density defined as $K_m = \frac{1}{2} \mu_0 M_S^2$, is considered. The magnet has a uniaxial magnetocrystalline anisotropy with $K_u = 0.1\ K_m$ and easy axis parrellel to the principle axis x_3 of the cube.

Flower and vortex state domains simulated using µ-Pro® Mag is plotted. Transition size, corresponding average magnetization, and energy densities are listed and compared with solutions submitted to the µMag group[14].
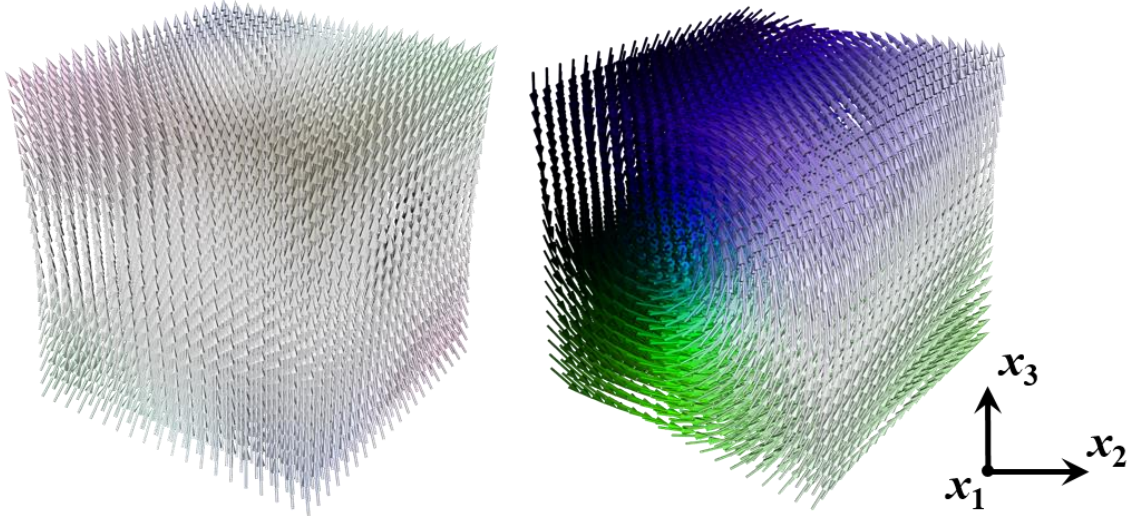
Figure 5.3 Stable flower state (left) and vortex state (right) magnetic domain structure in cubic magnet with L/l$_{ex}$ =8.40 and L/l$_{ex}$ =8.50, respectively.

Table 5.3 Transition size, average magnetization, and energy densities in the Flower and vortex structures, in μMag Standard Problem #3

	Length L/l$_{ex}$	Flower State				Vortex State			
		$<m_{x3}>$	$<f_{Demag}>$	$<f_{Exch}>$	$<f_{Ani}>$	$<m_{x1}>$	$<f_{Demag}>$	$<f_{Exch}>$	$<f_{Ani}>$
μ-Pro® Mag	8.46	0.97	0.2793	0.0177	0.0057	0.3543	0.0801	0.1703	0.0522
Rave[14]	8.46	0.971	0.2794	0.0177	0.0056	0.352	0.0783	0.1723	0.0521
Martins[14]	8.47	0.971	0.2792	0.0177	0.0056	0.3516	0.078	0.1724	0.0521
Hertel & Kronmüller[14]	8.52	0.973	0.2839	0.0158	0.0052	0.351	0.083	0.1696	0.0522

5.4 μMag Standard Problem #4

μMag Standard Problem #4 considers the magnetization dynamics in a of a 500nm × 125nm × 3nm permalloy magnet. The magnet is first relaxed to a equilibrium state by applying a saturating magnetic field along the [1, 1, 1] direction, which is then slowly reduced to zero. A magnetic field is further applied to reverse the magnetization, where the magnetization dynamics is assessed. The following material parameters are adopted:

$M_S = 8 \times 10^5$ A/m

$A = 1.3 \times 10^{-11}$ J/m

$K = 0$

$\alpha = 0.02$

$\gamma_0 = 2.211 \times 10^5$ m/(A.s)

Two switching events with different magnetic fields are considered:

Field (1): $\mu_0 H_x$ = -24.6 mT, $\mu_0 H_y$= 4.3 mT, $\mu_0 H_z$= 0.0 mT, which is approximately a 25mT field directly 170° counterclockwise from the positive x axis.
Field (2): $\mu_0 H_x$ = -35.5 mT, $\mu_0 H_y$= -6.3 mT, $\mu_0 H_z$= 0.0 mT, which is approximately a 36mT field directly 190° counterclockwise from the positive x axis.

Time sequence of magnetization during switching is modeled using μ-Pro® Mag. Results from both the implicit Gauss-Seidel projection method and the Runge Kutta method (RK4) for solution of the LLG equation are shown, both of which agree well with solutions submitted to the μMag group[14].
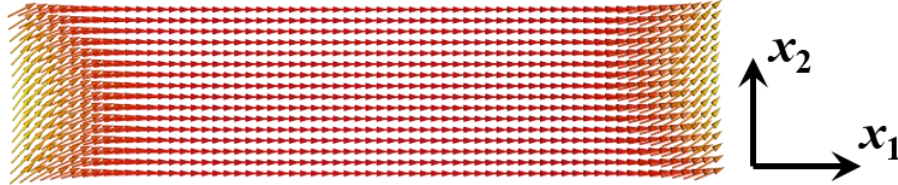
Figure 5.4.1 Initial magnetization distribution.
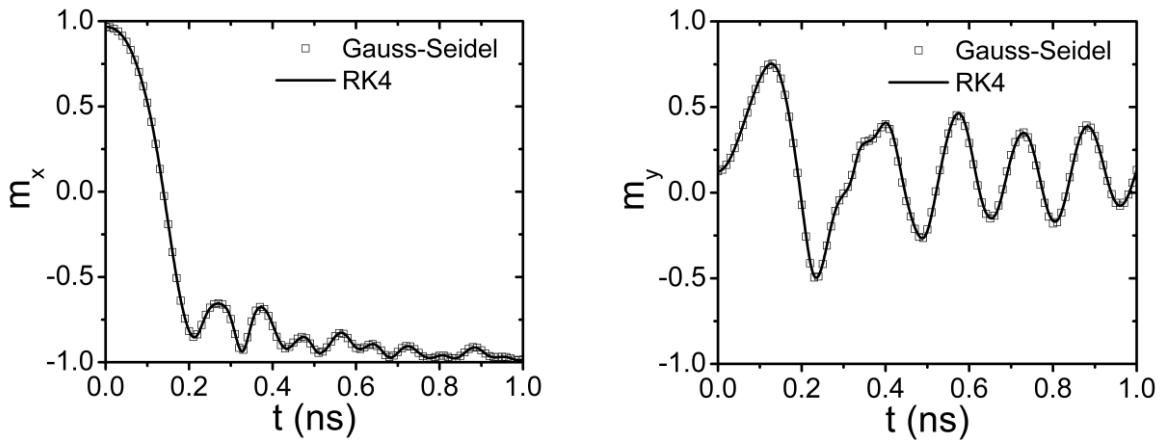
Figure 5.4.2 Time sequence of average magnetization on applying field (1).
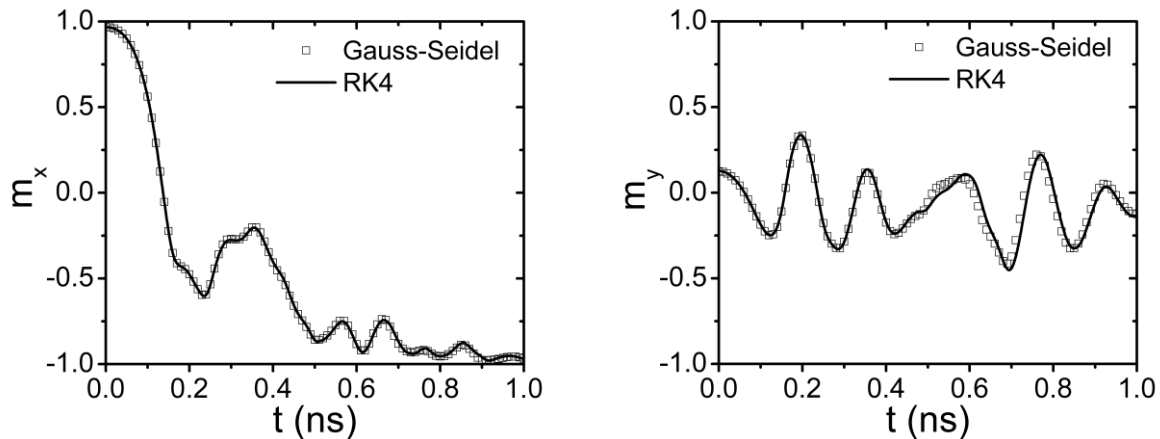
Figure 5.4.3 Time sequence of average magnetization on applying field (2).

5.5 μMag Standard Problem #5

μMag Standard Problem #5 considers effect the Zhang-Li spin-transfer-torque. A spin-polarized electric current of $j=10^{12}$ A/m along x_1 direction is applied to 100nm × 100nm × 10nm permalloy magnet with an initial vortex structure. The following parameters are adopted:

$M_S = 8 \times 10^5$ A/m
$A = 1.3 \times 10^{-11}$ J/m
$K = 0$
$\alpha = 0.1$
$\gamma_0 = 2.211 \times 10^5$ m/(A.s)

The obtained magnetic vortex structure and time-dependent average magnetization is shown below. It agrees well with the OOMMF solution.
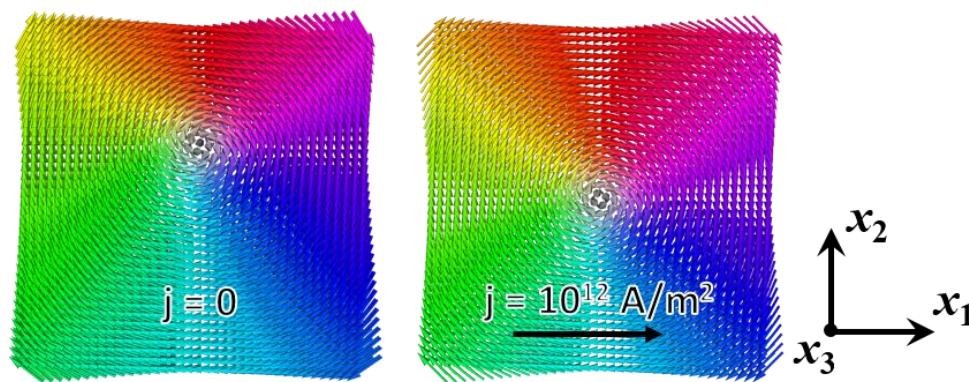
Figure 5.5.1 Initial vortex structure (left) and the vortex structure after applying the current for 5ns (right).
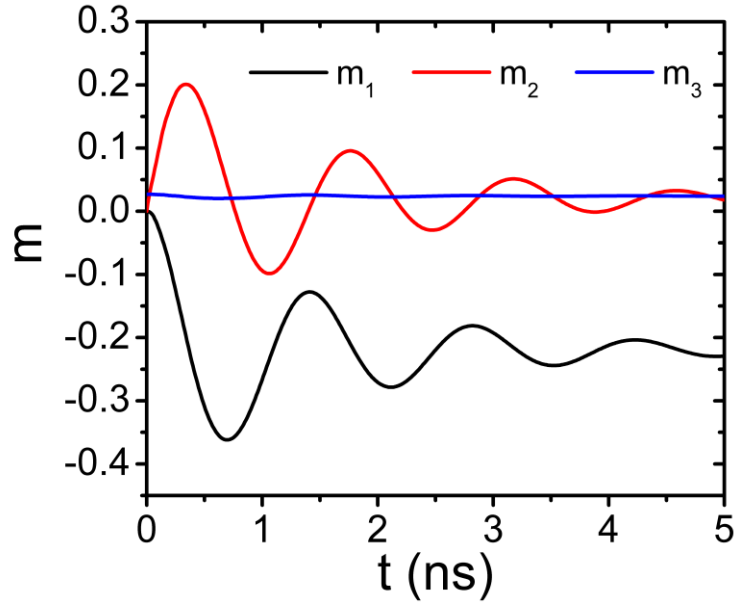
Figure 5.5.2 Time-dependent average magnetization under the applied electric current.

5.6 Strain-induced domain pattern in thin film

This example considers the relaxed magnetic domain structure of a 100nm-thick nickel thin film. The nickel is considered isotropic (no magnetocrystalline anisotropy), with the following parameters adopted:

$M_S = 4.85 \times 10^5$ A/m
$A = 8.2 \times 10^{-12}$ J/m
$K = 0$
$\alpha = 0.3$
$\gamma_0 = 2.42 \times 10^5$ m/(A.s)
$\lambda_{100} = \lambda_{111} = -32.9 \times 10^{-6}$
$c_{11} = 246.5$ GPa
$c_{12} = 147.3$ GPa
$c_{44} = 49.6$ GPa

The substrate is assumed to possess an elastic stiffness equal to the thin film magnet. The effect of biaxial substrate mismatch strains ε_S (= $\varepsilon_{11} = \varepsilon_{22}$) are investigated.

The obtained equilibrium magnetization distribution at $\varepsilon_S = 0.003$ and $\varepsilon_S = 0.004$ are shown below. The out of plane component of the magnetization is measured by calculating $<m_3^2>$ averaged throughout the sample, which shows a trend to increase with increasing ε_S.
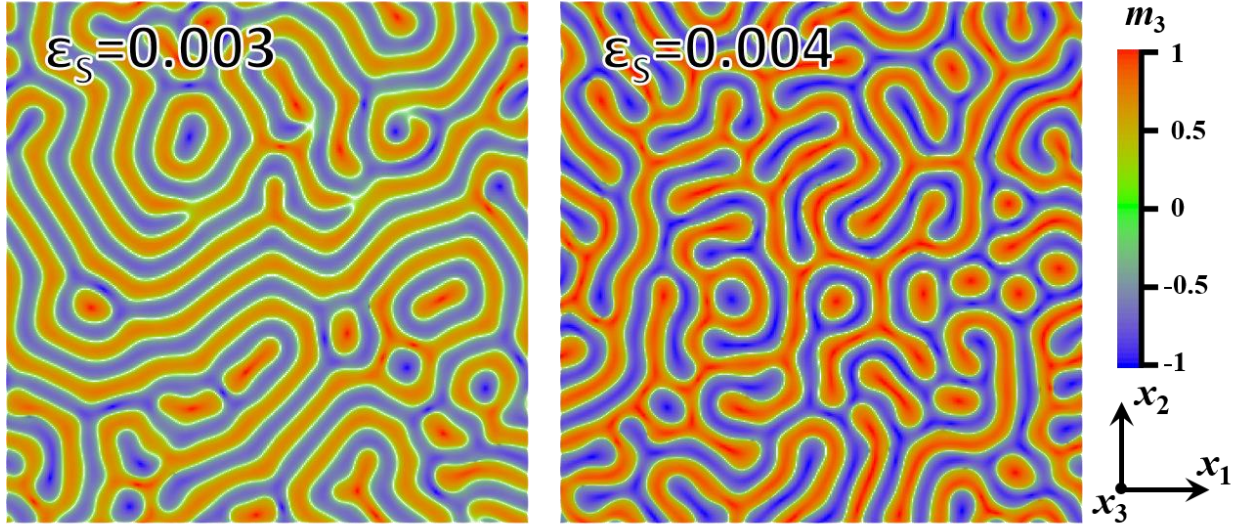
30

Figure 5.6.1 Equilibrium magnetization distribution, which shows striped out-of-plane domains with Neel type domain walls at $\varepsilon_S = 0.004$, and a similar structure with relatively smaller out-of-plane component at $\varepsilon_S = 0.003$.
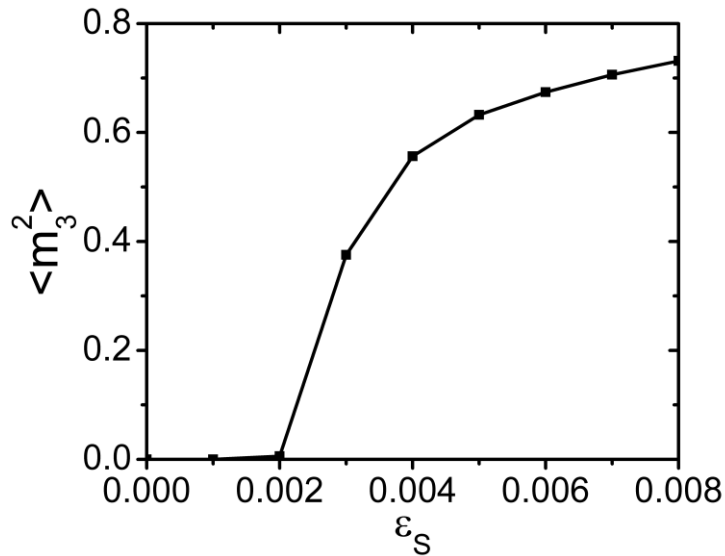

Figure 5.6.2 Average out-of-plane magnetization component $<m_3^2>$ of the equilibrium magnetization as a function of substrate strain ε_S. It shows that $<m_3^2>$ increases with increasing ε_S and dominates at $\varepsilon_S > 0.004$.

5.7 DMI

This is an example following the calculations in Ref. 15. It studies the transition of a Bloch wall to a Neel wall on increasing coefficient D of DMI, in a 300nm × 500nm × 0.6nm magnet with the following parameters adopted:

$M_S = 1.1 \times 10^6$ A/m

$A = 1.6 \times 10^{-11}$ J/m

$K_1 = 1.27 \times 10^6$ J/m^3 (Uniaxial anisotropy)

The obtained magnetic domain wall moments (the integrated magnetization m across the domain wall $\Phi_i = \int_{\text{across domain wall}} m_i dx_1$) as a function of D are shown below. It agrees well with the solutions given by q-Φ model[15] and MUMAX3[16].
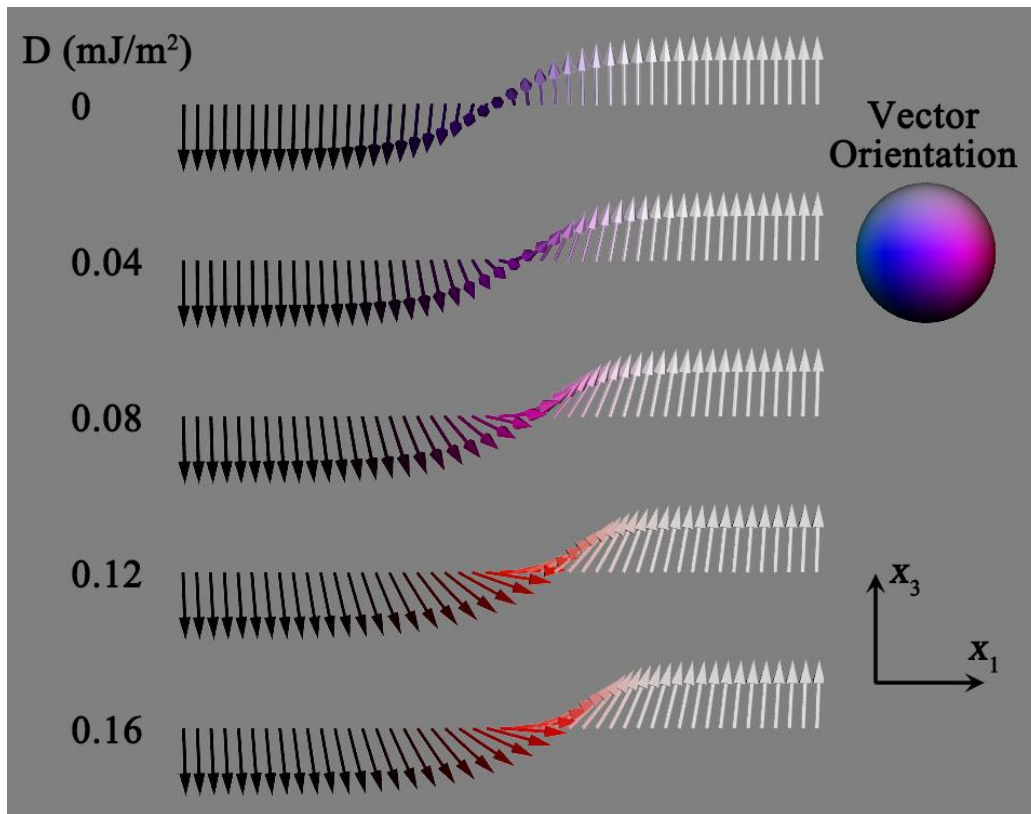

Figure 5.7.1 Simulated magnetization distribution across the domain wall.
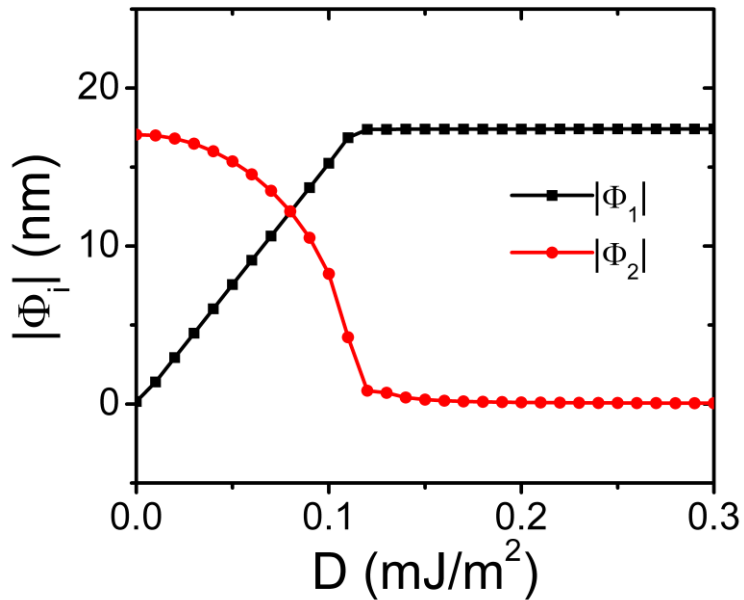
Figure 5.7.2 Simulated domain wall moments as a function of D.

5.8 Polycrystalline magnet

This example demonstrates the magnetic domain structure in a single crystal or polycrystalline 850nm (minor axis) × 2200nm (major axis) × 5nm (thickness) elliptical cylinder permalloy island with the following parameters adopted:

$M_S = 8.0 \times 10^5$ A/m

$A = 1.3 \times 10^{-11}$ J/m

Cubic magnetocrystalline anisotropy with different K_1 are used and compared with each other.
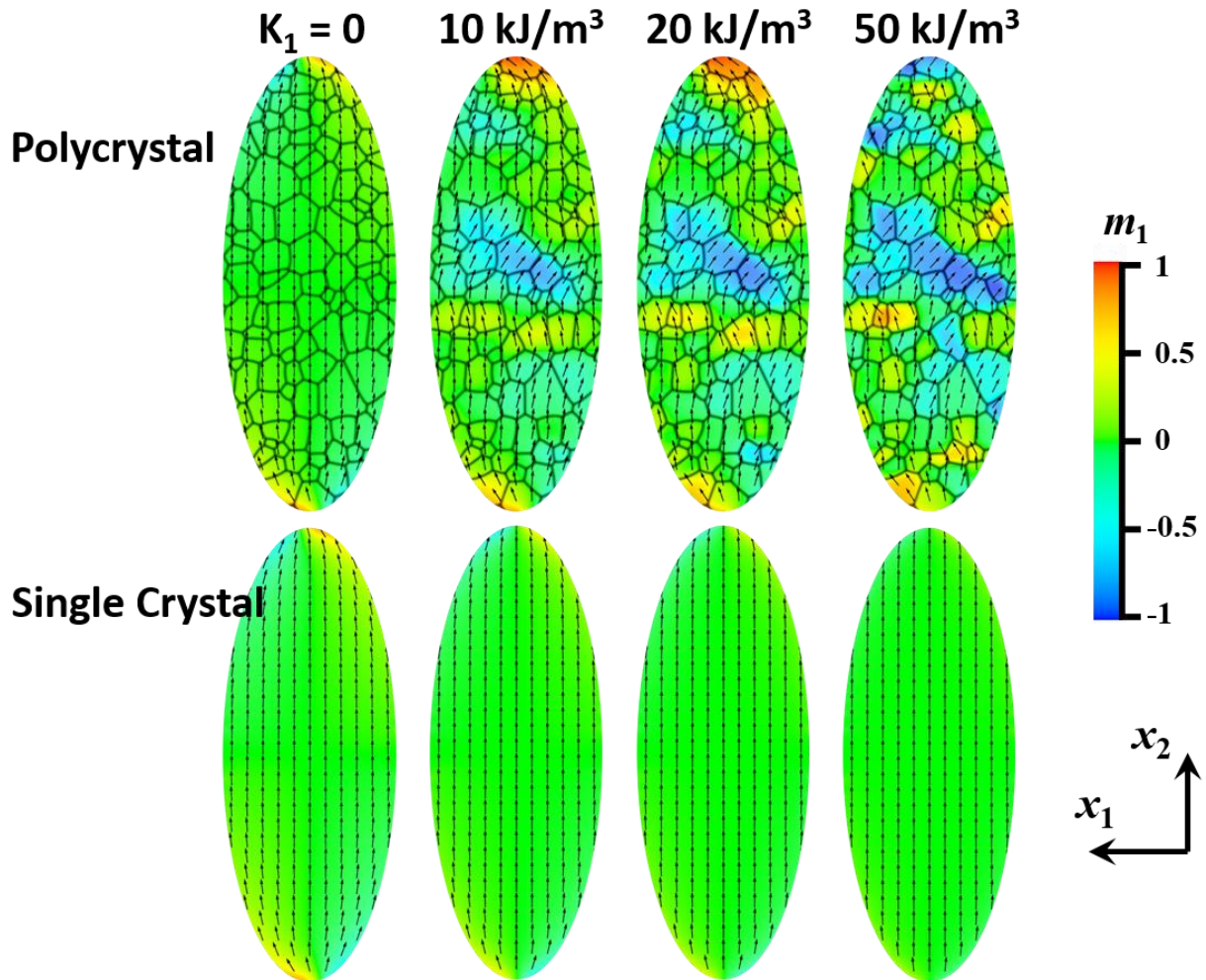
Figure 5.8 Simulated magnetization distribution in polycrystal and single crystal islands with different K_1.

5.9 Thermal fluctuation

This example tests the mean magnetization of a $(10nm)^3$ magnet with uniaxial magnetocrystalline anisotropy, which changes over time due to thermal fluctuation. The following parameters are adopted:

$M_S = 1.0 \times 10^6$ A/m

$K_1 = 1.0 \times 10^4$ J/m^3 (Uniaxial anisotropy)

$T = 100$ K

Effects of stray field and exchange interaction are neglected. A simulation system consisting of $256 \times 256 \times 1$ grid points with the size of $(10nm)^3$, which are independent from each other, is used to model the statistical mean.

The time-dependent average magnetization is modeled, which agrees well with the solution from MUMAX3.
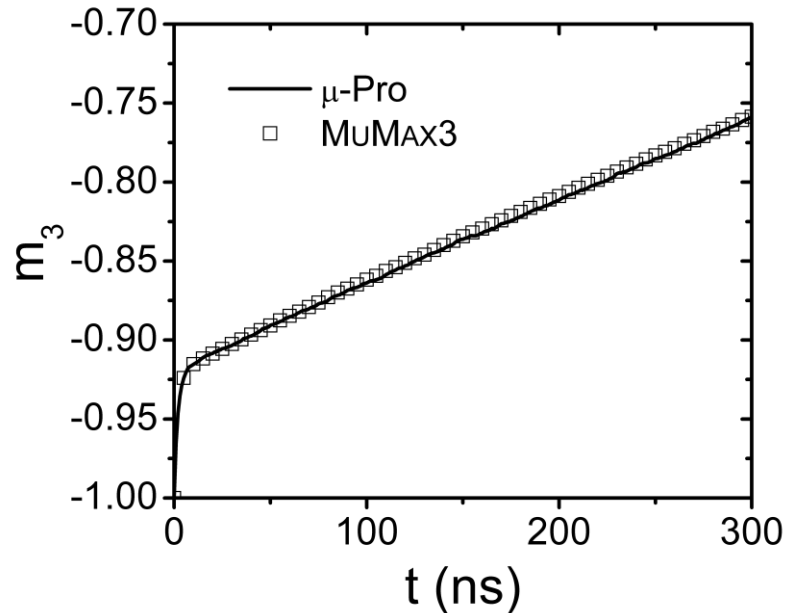
Figure 5.9 Simulated average magnetization sequence over time, compared with solution from MUMAX3.

References

[1]   X.-P. Wang, C. J. García-Cervera, and W. E, "A Gauss–Seidel Projection Method for Micromagnetics Simulations," *J. Comput. Phys.*, vol. 171, no. 1, pp. 357–372, Jul. 2001.

[2]   L.-Q. Chen and J. Shen, "Applications of semi-implicit Fourier-spectral method to phase field equations," *Comput. Phys. Commun.*, vol. 108, no. 2–3, pp. 147–158, 1998.

[3]   J. Zhang and L.-Q. Chen, "Phase-field microelasticity theory and micromagnetic simulations of domain structures in giant magnetostrictive materials," *Acta Mater.*, vol. 53, no. 9, pp. 2845–2855, May 2005.

[4]   K. Fabian and A. Kirchner, "Three-dimensional micromagnetic calculations for magnetite using FFT," *Geophys. J. ...*, pp. 89–104, 1996.

[5]   Y. Li, S. Y. Hu, Z.-K. Liu, and L.-Q. Chen, "Effect of substrate constraint on the stability and evolution of ferroelectric domain structures in thin films," *Acta Mater.*, vol. 50, pp. 395–411, 2002.

[6]   S. Y. Hu and L.-Q. Chen, "A phase-field model for evolving microstructures with strong elastic inhomogeneity," *Acta Mater.*, vol. 49, no. 11, pp. 1879–1890, Jun. 2001.

[7]   A. G. Khachaturyan, *Theory of Structural Transformation in Solids*. New York: Wiley, 1983.

[8]   J.-M. Hu, T. N. Yang, L.-Q. Chen, and C.-W. Nan, "Engineering domain structures in

nanoscale magnetic thin films via strain," *J. Appl. Phys.*, vol. 114, no. 16, p. 164303, 2013.

[9]   S. Rohart and A. Thiaville, "Skyrmion confinement in ultrathin film nanostructures in the presence of Dzyaloshinskii-Moriya interaction," *Phys. Rev. B - Condens. Matter Mater. Phys.*, vol. 88, no. 18, pp. 1–8, 2013.

[10]   G. Finocchio, M. Carpentieri, E. Martinez, and B. Azzerboni, "Switching of a single ferromagnetic layer driven by spin Hall effect," *Appl. Phys. Lett.*, vol. 102, no. 21, 2013.

[11]   J. C. Slonczewski, "Current-driven excitation of magnetic multilayers," *J. Magn. Magn. Mater.*, vol. 159, no. 1–2, pp. L1–L7, Jun. 1996.

[12]   L. Torres, L. Lopez-Diaz, E. Martinez, M. Carpentieri, and G. Finocchio, "Micromagnetic computations of spin polarized current-driven magnetization processes," *J. Magn. Magn. Mater.*, vol. 286, no. SPEC. ISS., pp. 381–385, 2005.

[13]   S. Zhang and Z. Li, "Roles of nonequilibrium conduction electrons on the magnetization dynamics of ferromagnets," *Phys. Rev. Lett.*, vol. 93, no. 12, pp. 1–4, 2004.

[14]   http://www.ctcms.nist.gov/~rdm/mumag.org.html

[15]   A. Thiaville, S. Rohart, E. Jué, V. Cros, and A. Fert, "Dynamics of Dzyaloshinskii domain walls in ultrathin magnetic films," *EPL*, vol. 100, no. 5, pp. 57002, 2012.

[16]   A. Vansteenkiste, J. Leliaert, M. Dvornik, M. Helsen, F. Garcia-Sanchez, and B. Van Waeyenberge, "The design and verification of MuMax3, " *AIP Adv.*, vol. 4, no. 10, pp. 0–22, 2014.